Lossy Electric Transmission Line Soft Fault Diagnosis: an Inverse Scattering Approach

Huaibin Tang, Qinghua Zhang

Lossy Electric Transmission Line Soft Fault Diagnosis: an Inverse Scattering Approach

Huaibin Tang and Qinghua Zhang

***Abstract*—In this paper, the diagnosis of soft faults in lossy electric transmission lines is studied through the inverse scattering approach. The considered soft faults are modeled as continuous spatial variations of distributed characteristic parameters of transmission lines. The diagnosis of such faults from reflection and transmission coefficients measured at the ends of a line can be formulated as an inverse problem. The relationship between this inverse problem and the inverse scattering theory has been studied by Jaulent in 1982 through transformations from the telegrapher's equations of transmission lines to Zakharov-Shabat equations. The present paper clarifies and completes the computation of the theoretic scattering data required by the inverse scattering transform from the practically measured engineering scattering data. The inverse scattering method is then applied to numerically simulated lossy transmission lines to confirm the feasibility of the studied approach to soft fault diagnosis.**

***Index Terms*—inverse scattering, lossy transmission line, soft fault diagnosis, telegrapher's equations, Zakharov-Shabat equations.**

I. Introduction

Today's engineering systems are heavily equipped with electric and electronic components, and consequently, the reliability of electric connections becomes a crucial issue. Among the efforts of developing reliable electric systems, a promising technology for transmission line fault diagnosis is the reflectometry, which consists in analyzing the reflection and the transmission of electric waves observed at the ends of a transmission line. For hard fault (open or short circuits) diagnosis, efficient reflectometry-based methods have been reported, for instance, [1]–[3]. However, the diagnosis of soft faults in transmission lines remains an open problem. It is reported in [4] that the reflections caused by weak impedance discontinuities at boundaries of faulty segments are comparable to or smaller than the effects of various noises and disturbances. Hence it is difficult to detect and to locate such faults.

The purpose of the present paper is to study a kind of soft faults corresponding to *smooth* variations of characteristic parameters in lossy transmission lines. The reflections caused by such faults may be even weaker than those caused by impedance discontinuities, but this problem is not addressed in this paper (hence it is assumed that reflection and transmission coefficients are sufficiently accurately measured, under good experimental conditions). Instead, the main issue here is the fact that the considered smooth soft faults cannot be simply located by the discontinuities of their boundaries, because they do not have such boundaries. The adopted approach treats the diagnosis problem as an inverse problem: given the reflectometry measurements made at the ends of a transmission line, namely the reflection and transmission coefficients, what are the distributed characteristic properties of the transmission line? This problem is strongly related to the inverse scattering transform (IST for short). For introductory presentations of the IST, we refer the readers to [5], [6]. Some early investigation on the application of the IST to transmission lines was reported in [7]. This topic then attracted the attention of many researchers in 1970's and 1980's. For solving the inverse problem of transmission lines, there exist two approaches. One is in time domain, as studied in [8], [9] with continuous and discrete transmission line models respectively. The other approach is in frequency domain, with its theoretic basis founded more than a quarter of a century ago by [10]. More recently, [11] studied multiconductor uniform transmission lines, and [12] investigated the application of the IST to finite length lossless transmission lines. To our knowledge, no practical application of the IST to general lossy transmission line fault diagnosis has been reported. The IST for transmission lines is usually studied under the assumption of *lossless* transmission lines ([12]), or by neglecting either ohmic loss or dielectric loss ([13], [14]). As losses have significant impacts on most real transmission lines, the lack of studies on the lossy case has been probably a major obstacle to the application of the IST to transmission lines.

In this paper, the application of the frequency domain IST to the general *lossy* transmission lines for soft fault diagnosis is studied. It extends the results of [12] to *lossy* transmission lines. This extension concerns several aspects. The relationship between finite length transmission lines and the IST defined on the infinite interval, which was already studied for lossless lines in [12], will be extended to lossy lines in this paper. In [10], the computation of the theoretic scattering data required by the IST from practically measure scattering data involves two unknown constants, namely the wave propagation time over the transmission line and an integral of the line characteristic parameters. It will be shown in this paper that the computation of the theoretic scattering data can be simplified so that these unknown constants are not required. The numerical inverse scattering algorithm for lossless lines used in [12] will also be extended to lossy lines in this paper.

This work has been supported by the ANR INSCAN (INfrastructure Safety Cables ANalysis).

H.T. and Q.Z. are with INRIA, Campus de Beaulieu, 35042 Rennes, France. Emails: hutang@irisa.fr, zhang@irisa.fr.

In order to illustrate the efficiency of the proposed method for transmission line soft fault diagnosis, results of numerical simulation are presented in this paper. To simulate reflectometry measurements, reflection and transmission coefficients are computed by solving the telegrapher's equations in the frequency domain. The simulated reflection and transmission coefficients are then fed to the inverse scattering algorithm which computes the two potential functions of the Zakharov-Shabat equations. Simulated spatial variations of the characteristic parameters, representing soft faults of the transmission line, can be revealed from the two potential functions computed by the inverse scattering algorithm.

This paper is organized as follows: In section 2, we present the formulation of the inverse scattering problem of lossy electric transmission lines. Section 3 presents our simulation results. Concluding remarks are made at section 4.

II. The inverse scattering problem for lossy transmission lines

In this section, we first shortly recall the transformations from telegrapher's equations to Zakharov-Shabat equations with two potential functions and describe the formulation of the related IST. This result initially derived by [10] is the theoretical basis for the inverse scattering problem of transmission lines in frequency domain. Considering its practical application, we then clarify and complete the computation of the theoretic scattering data required by the IST from the practically measured engineering scattering data.

A. The telegrapher's equations and the scattering data of lossy transmission lines

Consider a lossy transmission line which is connected to an alternating voltage source of frequency k and to a load (see Fig. 1), the voltage $U(k,z)$ and the current $I(k,z)$ at any point z are governed by the frequency domain telegrapher's equations [10]:

$$\frac{dU(k,z)}{dz} - ikL(z)I(k,z) + R(z)I(k,z) = 0 \quad \text{(1a)}$$

$$\frac{dI(k,z)}{dz} - ikC(z)U(k,z) + G(z)U(k,z) = 0 \quad \text{(1b)}$$

where i is the imaginary unit, $R(z) \geq 0$, $L(z) > 0, C(z) > 0$, and $G(z) \geq 0$ being respectively its series resistance, distributed inductance, capacitance, and shunt conductance (RLCG parameters for short) along the longitudinal axis z.

As shown in Fig. 1, let $z = 0$ and $z = z_l$ be the space coordinate values corresponding to the left and right ends of the finite length lossy transmission line. Denote with Z_S the source internal impedance and with Z_L the load impedance, then the measured left reflection coefficient is

$$r_{l_e}(k) = \frac{Z(k,0) - Z_S}{Z(k,0) + Z_S} = \frac{U(k,0) - Z_S I(k,0)}{U(k,0) + Z_S I(k,0)} \quad (2)$$

where $Z(k,0) = \dfrac{U(k,0)}{I(k,0)}$ is the input impedance of the transmission line. And the measured transmission coefficient is

$$t_e(k) = \frac{Z_L^{-\frac{1}{2}} U(k,z_l) + Z_L^{\frac{1}{2}} I(k,z_l)}{Z_S^{-\frac{1}{2}} U(k,0) + Z_S^{\frac{1}{2}} I(k,0)} \quad (3)$$

For the measurement of the right reflection coefficient, another experiment is made by inverting the source end and the load end, i.e., connecting the lossy transmission line to the source at the right end and to the load at the left end. For this experiment, we denote with Z'_S and Z'_L the source internal impedance and the load impedance, and with $U'(k,z)$, $I'(k,z)$ the voltage and current values for $z \in [0, z_l]$. Then the measured right reflection coefficient is

$$r_{r_e}(k) = \frac{Z'(k,z_l) + Z'_S}{Z'(k,z_l) - Z'_S} = \frac{U'(k,z_l) + Z'_S I'(k,z_l)}{U'(k,z_l) - Z'_S I'(k,z_l)} \quad (4)$$

where $Z'(k,z_l) = \dfrac{U'(k,z_l)}{I'(k,z_l)}$ is the (right end) input impedance of the transmission line.

In this paper, the source and load impedances are assumed to have real values.

As the left reflection coefficient r_{l_e}, transmission coefficient t_e, and right reflection coefficient r_{r_e} expressed in (2)-(4) correspond to the measurements used in engineering practice, they will be referred to as *engineering* scattering data (to be distinguished from the theoretic scattering data used in the inverse scattering theory, which will be introduced later in this paper). Their definitions are related to the S-parameters of transmission lines ([15], chapter 13).

B. From Telegrapher's equations to Zakharov-Shabat equations

Following [10], the Liouville transformation

$$x(z) = \int_0^z \sqrt{L(s)C(s)}ds$$

will be applied to replace the space coordinate z by the wave propagation time x in the telegrapher's equations. By abuse of notation, $R(x(z))$ will be simply written as $R(x)$, and similarly for $G(x), L(x), C(x), I(k,x)$, and $U(k,x)$. Let $x_1 = 0$ and $x_2 = l$ be the $x-$coordinate values corresponding to the left and right ends, as shown in Fig. 2. The value of l is known as the wave propagation time over the transmission line. Then the telegrapher's equations (1) become

$$\frac{dU(k,x)}{dx} = \left[ik - \frac{R(x)}{L(x)}\right] Z_0(x) I(k,x) \quad \text{(5a)}$$

$$\frac{dI(k,x)}{dx} = \left[ik - \frac{G(x)}{C(x)}\right] Z_0^{-1}(x) U(k,x) \quad \text{(5b)}$$

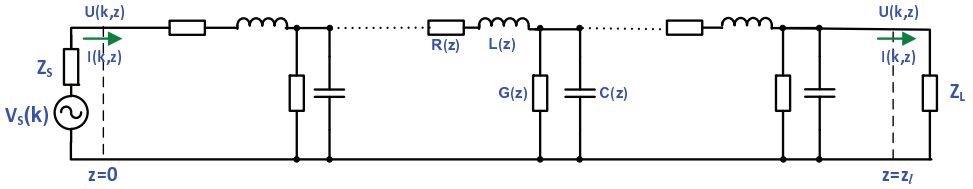

Fig. 1. The lossy transmission line is connected to an alternating voltage source of frequency k at the left end and to a load at the right end (see Fig. 1). This circuit diagram is for measuring the left reflection coefficient $r_{l_e}(k)$ and transmission coefficient $t_e(k)$.

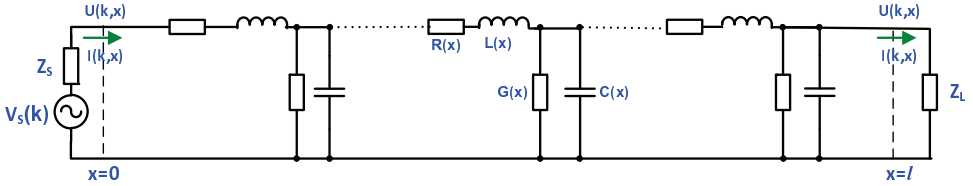

Fig. 2. The circuit of Fig. 1 re-illustrated in $x-$coordinate.

where

$$Z_0(x) = \sqrt{\frac{L(x)}{C(x)}} \tag{6}$$

In the lossless case, i.e., $R(x) = G(x) = 0$, $Z_0(x)$ is equal to the characteristic impedance of the line at the point x.

Define two new variables

$$\nu_1(k,x) = \frac{1}{2}\left[Z_0^{-\frac{1}{2}}(x)U(k,x) - Z_0^{\frac{1}{2}}(x)I(k,x)\right] \tag{7a}$$

$$\nu_2(k,x) = \frac{1}{2}\left[Z_0^{-\frac{1}{2}}(x)U(k,x) + Z_0^{\frac{1}{2}}(x)I(k,x)\right] \tag{7b}$$

which are respectively known as the *reflected wave* propagating in the negative x direction and the incident wave propagating in the positive x direction. Then equations (5) lead to the following Zakharov-Shabat equations with *three* potential functions:

$$\frac{d\nu_1(k,x)}{dx} + ik\nu_1(k,x) = q_3(x)\nu_1(k,x) + q^+(x)\nu_2(k,x) \tag{8a}$$

$$\frac{d\nu_2(k,x)}{dx} - ik\nu_2(k,x) = q^-(x)\nu_1(k,x) - q_3(x)\nu_2(k,x) \tag{8b}$$

with the three potential functions [1]

$$\begin{aligned} q^{\pm}(x) &= -\frac{1}{4}\frac{d}{dx}\left[\ln\frac{L(x)}{C(x)}\right] \mp \frac{1}{2}\left[\frac{R(x)}{L(x)} - \frac{G(x)}{C(x)}\right] \\ &= -\frac{1}{2Z_0(x)}\frac{d}{dx}Z_0(x) \mp \frac{1}{2}\left[\frac{R(x)}{L(x)} - \frac{G(x)}{C(x)}\right] \end{aligned} \tag{9a}$$

$$q_3(x) = \frac{1}{2}\left[\frac{R(x)}{L(x)} + \frac{G(x)}{C(x)}\right] \tag{9b}$$

To guarantee the continuous property of the potential functions, we make the following assumption:

Assumption 1. *For x ranging within the transmission line, the functions $R(x)$ and $G(x)$ are continuous, and the functions $L(x)$ and $C(x)$ are sufficiently regular real functions such that $Z_0(x)$ defined in* (6) *has a continuous derivative.*

These *three*-potential equations are further reduced by defining

$$\tilde{\nu}_1(k,x) = \nu_1(k,x)e^{-\int_{-\infty}^{x} q_3(y)dy} \tag{10a}$$

$$\tilde{\nu}_2(k,x) = \nu_2(k,x)e^{\int_{-\infty}^{x} q_3(y)dy} \tag{10b}$$

which satisfy the following Zakharov-Shabat equations with *two* potential functions (referred to as ZS$^+(k)$)

$$\text{ZS}^+(k)\text{:} \begin{cases} \dfrac{d\tilde{\nu}_1(k,x)}{dx} + ik\tilde{\nu}_1(k,x) = \tilde{q}^+(x)\tilde{\nu}_2(k,x) & \text{(11a)} \\ \dfrac{d\tilde{\nu}_2(k,x)}{dx} - ik\tilde{\nu}_2(k,x) = \tilde{q}^-(x)\tilde{\nu}_1(k,x) & \text{(11b)} \end{cases}$$

with the two potential functions

$$\tilde{q}^{\pm}(x) = q^{\pm}(x)e^{\mp 2\int_{-\infty}^{x} q_3(y)dy} \tag{12}$$

As a comparison, in the case of *lossless* transmission lines, as studied in [12], these two different potential functions are equal. The above Zakharov-Shabat equations with *two* potential functions (11) have been studied in the inverse scattering theory [6]. Based on the related IST, it is possible to compute the potential functions $\tilde{q}^{\pm}(x)$ from the scattering data (reflectometry measurements) in the case of lossy transmission lines. Thus, through the relations between the potential functions $\tilde{q}^{\pm}(x)$ and the $RLCG$ parameters of the transmission line formulated in (9) and (12), distributed

[1]It is noted that, for a better agreement with the engineering definition of scattering data which will be reminded later, $\nu_1(k,x)$ and the potential functions $q^{\pm}(x)$ differ by a negative sign from the corresponding notations in [10].

properties of lossy electric transmission lines can be retrieved.

C. The relation between the theoretic scattering data and the engineering scattering data

Let $r_l(k)$, $t(k)$, and $r_r(k)$ denote the left reflection coefficient, transmission coefficient, and right reflection coefficient (referred to as scattering data) for the Zakharov-Shabat equations with three potential functions (8). As stated in [10], it is known that these scattering data can be expressed as follows

$$r_l(k) = \lim_{x\to-\infty} \frac{f_{l1}(k,x)}{f_{l2}(k,x)} e^{2ikx} \tag{13a}$$

$$t(k) = \frac{\lim\limits_{x\to+\infty} f_{l2}(k,x)e^{-ikx}}{\lim\limits_{x\to-\infty} f_{l2}(k,x)e^{-ikx}} = \frac{\lim\limits_{x\to-\infty} f_{r1}(k,x)e^{ikx}}{\lim\limits_{x\to+\infty} f_{r1}(k,x)e^{ikx}} \tag{13b}$$

$$r_r(k) = \lim_{x\to+\infty} \frac{f_{r2}(k,x)}{f_{r1}(k,x)} e^{-2ikx} \tag{13c}$$

where $f_l(k,x)$ and $f_r(k,x)$ are the right and left Jost solutions to (8) satisfying

$$\lim_{x\to+\infty} \begin{pmatrix} f_{l1}(k,x) \\ e^{-ikx} f_{l2}(k,x) \end{pmatrix} = \begin{pmatrix} 0 \\ 1 \end{pmatrix} \tag{14}$$

$$\lim_{x\to-\infty} \begin{pmatrix} e^{ikx} f_{r1}(k,x) \\ f_{r2}(k,x) \end{pmatrix} = \begin{pmatrix} 1 \\ 0 \end{pmatrix} \tag{15}$$

To relate the engineering scattering data r_{l_e}, r_{r_e}, and t_e to the theoretic scattering data r_l, r_r, and t, the first difficulty is due to the fact that the former is defined at the ends of a finite length transmission line, whereas the latter is related to the limiting behaviors of Jost solutions of (11) at infinity. To solve this problem, the finite length transmission line will be extended (with arbitrarily long extra line segments) in a way such that the voltage and the current remain unchanged in the original part of the transmission line. It will be further shown that, for such an (infinitely) extended line, the limiting values of the ratios expressed in (13) can be simply assessed at ends of the segment corresponding to the original line, namely at $x = 0$ and $x = l$.

Proposition 1. *Consider a lossy transmission line connected to a source with the internal impedance Z_S at its left end and to a load with the impedance Z_L at its right end, as illustrated in Fig. 2. As shown in Fig. 3, we extend the original circuit as follows:*

- *insert a uniform lossless transmission line (represented by dashed lines in Fig. 3) of length a with $R(x) = 0$, $G(x) = 0$, and the characteristic impedance (as defined in* (6)*) $Z_0(x) = Z_S$ between the source and the left end of the original circuit;*
- *insert a uniform lossless transmission line (represented by dashed lines in Fig. 3) of length b with $R(x) = 0$, $G(x) = 0$, and the characteristic impedance $Z_0(x) = Z_L$ between the right end of the original circuit and the load;*
- *add a phase shift $-ka$ to the source voltage.*

Then for any positive values of a and b, this extended circuit is equivalent to the original one, in the sense that they have the same values of $U(k,x)$ and $I(k,x)$ for any $x \in [0,l]$.

The proof of this result is similar to the proof of Proposition 1 in [12]. Thus the finite length line can be treated as if it was infinitely extended.

Similarly, the same result holds when the source end and the load end are inverted.

Proposition 2. *The relationship between the engineering scattering data and theoretic scattering data to the Zakharov-Shabat equations* (8) *are as follows:*

$$r_l(k) = r_{l_e}(k) \tag{16a}$$

$$t(k) = t_e(k)e^{-ikl} \tag{16b}$$

$$r_r(k) = r_{r_e}(k)e^{-2ikl} \tag{16c}$$

For the compactness of this paper, we put the proof of Proposition 2 in the Appendix at the end of this paper.

The result presented in Proposition 2 indicates that the theoretical scattering data of the Zakharov-Shabat equations (8) are identical, up to phase shifts which are related to the wave propagation time over the transmission line, to the scattering data of the transmission lines used in electrical engineering.

Remark 1. *For the extended circuit shown in Fig. 3, to ensure the continuity of the potential functions as formulated by* (9) *of the extended circuit for $x \in (-a, l+b)$, $R(x)$, $G(x)$, and the derivative of $Z_0(x)$ should be smooth at the two connection points $x = 0$ and $x = l$, which need the following assumption.*

Assumption 2. *The RLCG parameters of the transmission line at its left and right ends satisfy that*

$$\lim_{x\to0^+} R(x) = \lim_{x\to l^-} R(x) = 0$$
$$\lim_{x\to0^+} G(x) = \lim_{x\to l^-} G(x) = 0$$
$$\lim_{x\to0^+} \frac{dZ_0(x)}{dx} = \lim_{x\to l^-} \frac{dZ_0(x)}{dx} = 0$$

and we chose that the source internal impedance and the load locally matched to the characteristic impedance of the ends of the line, i.e.,

$$Z_S = \lim_{x\to0^+} Z_0(x), \quad Z_L = \lim_{x\to l^-} Z_0(x)$$

It is noted that Assumption 2 is not necessary for Proposition 2, but it ensures potential function regularities for all $x \in (-\infty, \infty)$ required by the IST. In practice, this assumption is not satisfied, since the ohmic and dielectric losses do not tend to zero at the ends of transmission lines. However, as shown in our simulation results, the discontinuities caused by

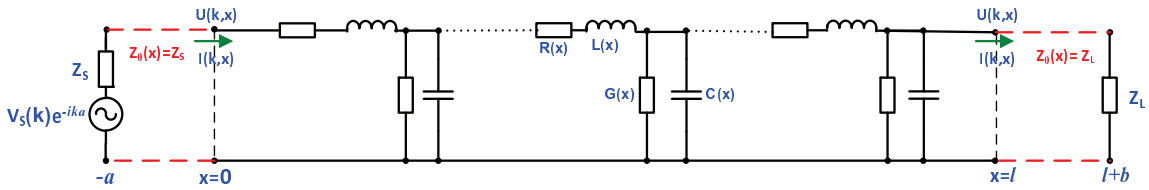

Fig. 3. Extended circuit diagram of Fig. 2 with the method presented in Proposition 1, by inserting uniform lossless transmission lines between the source, the load, and the corresponding ends of the original circuit and shifting the source phase by $-ka$.

typical losses are well tolerated by our numerical IST algorithm.

D. The inverse scattering algorithm for ZS$^+$(k)

For the extended circuit shown in Fig. 3, it can be easily checked that the potential functions $\tilde{q}^{\pm}(x)$ for $x \in (-a, 0)$ are equal to zeros. It then follows that, when $a \to +\infty$, $\tilde{q}^{\pm}(x) = 0$ for $x < 0$. The values of $\tilde{q}^{\pm}(x)$ for $x \geq 0$ can be computed from the scattering data through the inverse scattering algorithm, as presented in the following.

To retrieve the potential functions $\tilde{q}^{\pm}(x)$ from the scattering data only, it is assumed that the Zakharov-Shabat equations (11) have no bound state (square integrable solution for $x \in \mathbb{R}$). The IST computation requires the left reflection coefficient $\tilde{r}_l(k)$ of ZS$^+(k)$, and also the left reflection coefficient $\tilde{r}_l^-(k)$ of the *auxiliary* Zakharov-Shabat equations

$$\text{ZS}^-(k): \begin{cases} \dfrac{d\tilde{\nu}_1^-(k,x)}{dx} + ik\tilde{\nu}_1^-(k,x) \\ \qquad = \tilde{q}^-(x)\tilde{\nu}_2^-(k,x) & \text{(17a)} \\ \dfrac{d\tilde{\nu}_2^-(k,x)}{dx} - ik\tilde{\nu}_2^-(k,x) \\ \qquad = \tilde{q}^+(x)\tilde{\nu}_1^-(k,x) & \text{(17b)} \end{cases}$$

which are obtained by interchanging the two potential functions of ZS$^+(k)$.

Remark that $\tilde{r}_l(k)$ is the left reflection coefficient of the *two*-potential Zakharov-Shabat equations ZS$^+(k)$, which may be different from the left reflection coefficient $r_l(k)$ of the *three*-potential Zakharov-Shabat equations (8). Moreover, the auxiliary Zakharov-Shabat equations (17) do not physically exist. Hence the reflection coefficient $\tilde{r}_l^-(k)$ cannot be directly measured. In [10], these two reflection coefficients $\tilde{r}_l(k)$ and $\tilde{r}_l^-(k)$ are linked to the scattering data of the three-potential Zakharov-Shabat equations, namely $r_l(k), r_r(k)$, and $t(k)$ through the following equalities

$$\tilde{r}_l(k) = r_l(k) \quad \text{(18a)}$$

$$\tilde{t}(k) = t(k)e^{\int_{-\infty}^{+\infty} q_3(y)dy} \quad \text{(18b)}$$

$$\tilde{r}_r(k) = r_r(k)e^{2\int_{-\infty}^{+\infty} q_3(y)dy} \quad \text{(18c)}$$

and

$$\tilde{r}_l^-(k) = \left\{ \frac{\tilde{r}_r(k)}{\tilde{r}_r(k)\tilde{r}_l(k) - [\tilde{t}(k)]^2} \right\}^* \quad \text{(19)}$$

where " $*$" represents the complex conjugate.

It then seems possible to compute $\tilde{r}_l(k)$ and $\tilde{r}_l^-(k)$ from $r_l(k)$, $t(k)$, and $r_r(k)$, which are in turn related to the practically measured engineering scattering data $r_{l_e}(k), t_e(k)$, and $r_{r_e}(k)$ through (16). However, these computations require the knowledge of transmission line length l (in x-coordinate) and the integral value $\int_{-\infty}^{+\infty} q_3(y)dy$, which are unknown values in practice. Fortunately, as shown in the following proposition, $\tilde{r}_l(k)$ and $\tilde{r}_l^-(k)$ are directly linked to the engineering scattering data, without requiring the two unknown constants.

Proposition 3. *The theoretic scattering data for IST computations, namely, $\tilde{r}_l(k)$ and $\tilde{r}_l^-(k)$, can be calculated from the engineering scattering data as follows*

$$\tilde{r}_l(k) = r_{l_e}(k) \quad \text{(20a)}$$

$$\tilde{r}_l^-(k) = \left\{ \frac{r_{r_e}(k)}{r_{r_e}(k)r_{l_e}(k) - [t_e(k)]^2} \right\}^* \quad \text{(20b)}$$

Proof: (20a) can be proved directly by combing (18a) with (16a).

Now let us prove (20b). Substituting (18), (16) into (19),

$$\begin{aligned} \tilde{r}_l^-(k) &= \left\{ \frac{\tilde{r}_r(k)}{\tilde{r}_r(k)\tilde{r}_l(k) - [\tilde{t}(k)]^2} \right\}^* \\ &= \left\{ r_r(k)e^{2\int_{-\infty}^{+\infty} q_3(y)dy} \Big/ \Big\{ r_r(k)e^{2\int_{-\infty}^{+\infty} q_3(y)dy} \right. \\ &\qquad \left. \times r_l(k) - [t(k)e^{\int_{-\infty}^{+\infty} q_3(y)dy}]^2 \Big\} \right\}^* \\ &= \left\{ \frac{r_r(k)}{r_r(k) \times r_l(k) - [t(k)]^2} \right\}^* \\ &= \left\{ r_{r_e}(k)e^{-2ikl} \Big/ \Big\{ r_{r_e}(k)e^{-2ikl} \times r_{l_e}(k) \right. \\ &\qquad \left. - [t_e(k)e^{-ikl}]^2 \Big\} \right\}^* \end{aligned}$$

thus the result expressed in (20b) is obtained. ■

Proposition 3 indicates that the theoretic scattering data $\tilde{r}_l(k)$ and $\tilde{r}_l^-(k)$ required for the IST computation, can be computed directly from the engineering scattering data. This result completes the result of [10], which required the knowledge of the integral $\int_{-\infty}^{+\infty} q_3(y)dy$ for connecting $\tilde{r}_l(k)$ and $\tilde{r}_l^-(k)$ to the scattering data $r_l(k), t(k)$, and $r_r(k)$ of the three-potential Zakharov-Shabat equations, which would in

turn require the wave propagation time l to be connected to the engineering scattering data.

The IST consists of the following steps:

1) Compute the Fourier transforms

$$R_l(y) = \frac{1}{2\pi}\int_{-\infty}^{+\infty} \tilde{r}_l(k)e^{-iky}dk \tag{21a}$$

$$R_l^-(y) = \frac{1}{2\pi}\int_{-\infty}^{+\infty} \tilde{r}_l^-(k)e^{-iky}dk \tag{21b}$$

2) Solve the Gel'fand-Levitan-Marchenko (GLM) integral equations for the unknown kernels $A_{r1}(x,y)$, $A_{r2}(x,y)$, $A_{r1}^-(x,y)$, and $A_{r2}^-(x,y)$ in the half plane $x \le y$

$$\begin{aligned} &A_{r1}^-(x,y) + \int_{-y}^{x} dsR_l(y+s)A_{r2}(x,s) = 0 \\ &A_{r2}^-(x,y) + R_l(y+x) \\ &\qquad + \int_{-y}^{x} dsR_l(y+s)A_{r1}(x,s) = 0 \end{aligned}$$

$$\begin{aligned} &A_{r1}(x,y) + \int_{-y}^{x} dsR_l^-(y+s)A_{r2}^-(x,s) = 0 \\ &A_{r2}(x,y) + R_l^-(x+y) \\ &\qquad + \int_{-y}^{x} dsR_l^-(y+s)A_{r1}^-(x,s) = 0 \end{aligned}$$

3) Compute the potential functions $\tilde{q}^{\pm}(x)$ from

$$\tilde{q}^+(x) = 2A_{r2}^-(x,x), \quad \tilde{q}^-(x) = 2A_{r2}(x,x)$$

For more details about the above IST, we refer the readers to [6]. [2]

For the single-potential Zakharov-Shabat equations, efficiency numerical methods can be found in [16]–[18]. For two-potential Zakharov-Shabat equations, the numerical algorithm implementing this IST used in our simulation studies is described in [19] and can be seen as an extension of [16]. Both the algorithm in [19] and the one of [14] can produce similar results in our simulation studies, but the former is much faster.

III. Simulation Study

In this section, after presenting a numerical simulator to generate the scattering data of lossy transmission lines, we present some simulation results to confirm the validity of our numerical method.

[2]It is noted that our GLM integral equations are with finite integral intervals, differing to the GLM equations in [6] with infinite integral intervals. The transmission lines that we consider in this paper are causal systems, thus $R_l(y)$ and $R_l^-(y)$ respectively the time domain reflectograms at the left end and at the right end, are equal to zeros for $y < 0$. In this case, the GLM equations in [6] are reduced to finite integral intervals.

A. Numerical simulator for scattering data

For the transmission line shown in Fig. 2, if the value of $I(k,l)$ at the load end, say I_L, was known, then $U(k,l) = Z_L I_L$, and the telegrapher's equations (5) could be integrated reversely from $x = l$ to $x = 0$. It is clear that $U(k,x)$ and $I(k,x)$ depend linearly on I_L. Then it can be readily seen that the left reflection coefficient $r_{l_e}(k)$ computed through (2) is independent of the actual value of I_L. Hence the arbitrary value of $I_L = 1$ can always be used for computing $r_{l_e}(k)$. Similarly, the transmission coefficient $t_e(k)$ and the right reflection coefficient $r_{r_e}(k)$ can also be computed with (3) and (4).

The above computations were made for a given value of k. We can repeat these computations with different values of k to cover a sufficiently large spectrum.

B. Simulation results

Consider a lossy transmission line of length $1km$ with $L(z) = 0.9\mu H/m$ and $C(z) = 0.1nF/m$ (constant values). After being converted to the x-coordinate, $l = 9.4868\mu s, L(x) = 94.8683H/s$, and $C(x) = 0.0105F/s$. To simulate soft faults affecting the lossy properties of the line, variations of $R(x)$ and $G(x)$ are introduced such that the R/L and G/C ratios are as depicted in Fig. 4. The numeric simulator as described in section III-A is first implemented to generate the engineering reflection and transmission coefficients $r_{l_e}(k), r_{r_e}(k)$, and $t_e(k)$. The simulated results are depicted in Fig. 5 and Fig. 6. We can find that as k tends to infinity, $|t_e(k)|$ tends to a constant less than 1, which confirms the lossy properties of the transmission line. Then the scattering data $\tilde{r}_l(k)$ and $\tilde{r}_l^-(k)$ are computed through (20). After that, the numeric IST algorithm [19] is applied to compute the two potential functions $\tilde{q}^{\pm}$ from $\tilde{r}_l(k)$ and $\tilde{r}_l^-(k)$. As shown in Fig. 7, the result of IST accords well with the "true" potential functions $\tilde{q}^{\pm}$ directly simulated from (9) and (12).

The above simulation example has been made under Assumption 2, i.e. the resistance R and conductance G vanish at the two ends of the transmission line. As it is not realistic to assume vanishing R and G parameters, let us modify the simulation example so that R/L and G/C are as depicted in Fig. 8 and the parameters L and C remain the same as in the above example. The simulated engineering scattering data are shown in Fig. 9 and Fig. 10. As presented in Fig. 11, though Assumption 2 does not hold, the result of IST accords well with the "true" potential functions $\tilde{q}^{\pm}$ directly simulated from (9) and (12) except for slight oscillations close to the two ends. This simulation result shows that our numerical method is tolerant of weak violation of the continuity condition on R and G parameters stated in Assumption 2.

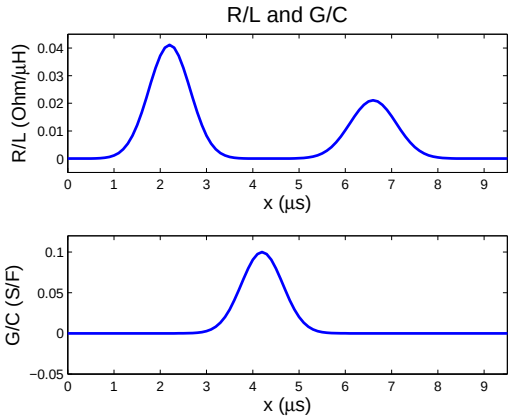

Fig. 4. Simulated R/L and G/C when R and G vanish at the ends of the transmission line.

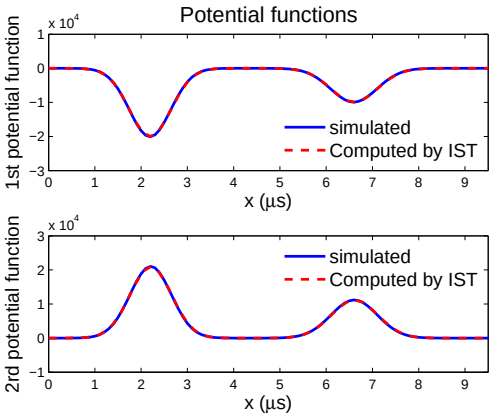

Fig. 7. $\tilde{q}^{\mp}$ computed by IST, and compared with the direct simulation for R/L and G/C depicted in Fig. 4. The two curves may not be distinguishable if printed in black and white.

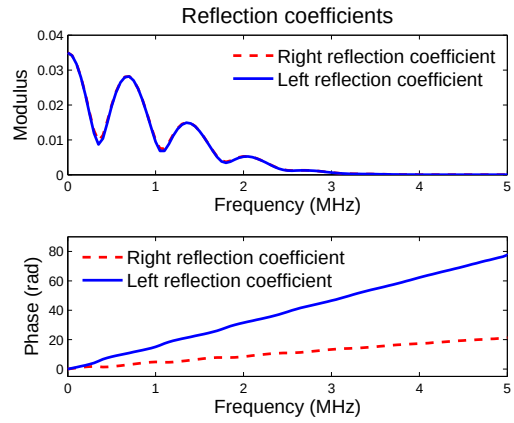

Fig. 5. Simulated engineering reflection coefficients $r_{l_e}(k)$ and $r_{r_e}(k)$ for R/L and G/C depicted in Fig. 4.

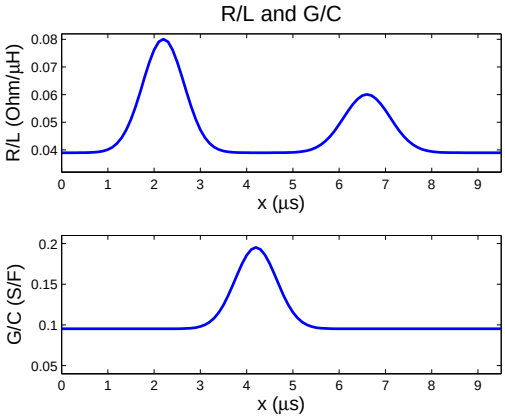

Fig. 8. Simulated R/L and G/C when R and G tend to positive constants at the ends of the transmission line.

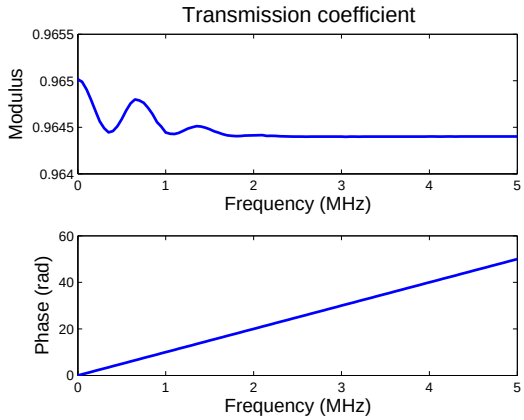

Fig. 6. Simulated engineering transmission coefficient $t_e(k)$ for R/L and G/C depicted in Fig. 4.

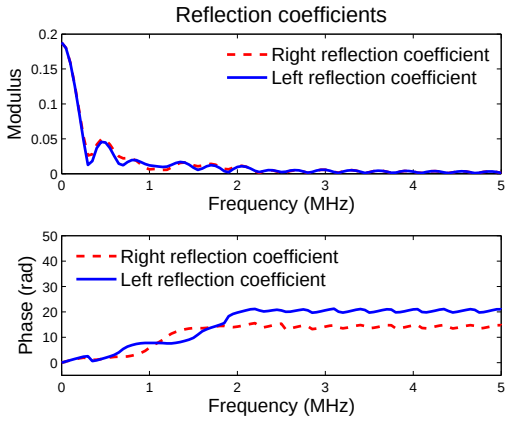

Fig. 9. Simulated engineering reflection coefficients $r_{l_e}(k)$ and $r_{r_e}(k)$ for R/L and G/C depicted in Fig. 8.

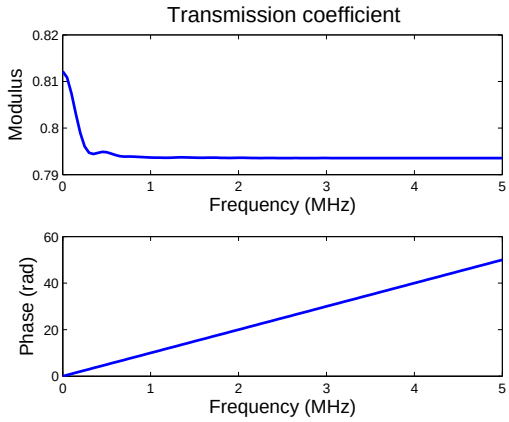

Fig. 10. Simulated engineering transmission coefficient $t_e(k)$ for R/L and G/C depicted in Fig. 8.

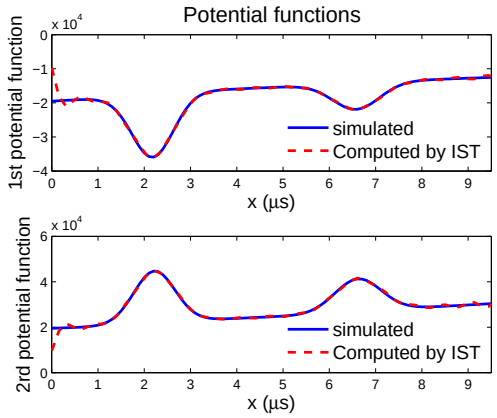

Fig. 11. $\tilde{q}^{\mp}$ computed by IST, and compared with the direct simulation for R/L and G/C depicted in Fig. 8. The results accord well except for slight oscillations close to the ends.

C. Remarks

From the simulation results, the values of the engineering reflection coefficients $r_{r_e}(k)$ and $r_{l_e}(k)$ are close to 0 after 5 MHz, thus we can use the truncated scattering data.

As the potential functions $\tilde{q}^{\pm}(x)$ are real, $\tilde{r}_l(-k) = [\tilde{r}_l(k)]^*$ and $\tilde{r}_l^-(-k) = [\tilde{r}_l^-(k)]^*$. It is then sufficient to simulate reflection coefficients $\tilde{r}_l(k)$ and $\tilde{r}_l{}^-(k)$ for positive values of k, though the integrals (21) range from $-\infty$ to $+\infty$.

IV. Conclusion

In this paper, based on the theoretic basis for the IST of the general lossy electric transmission lines established in [10], which relates the telegrapher's equations to the Zakharov-Shabat equations with two potential functions, we have studied the soft fault diagnosis of such lines by clarifying and completing the computation of the theoretic scattering data required by the IST from the practically measured engineering scattering data. Also, our simulation results confirm the feasibility of this approach. Since the potential functions $\tilde{q}^{\pm}(x)$ represent two functional relations between the three quotients of the parameters of the transmission line $L/C, R/L$, and G/C, these quotients cannot be uniquely determined from the two potential functions. However, the knowledge of $\tilde{q}^{\pm}(x)$ can reveal most faults causing distributed variations of RLCG parameters. If it is assumed that $R = 0$ (resp. $G = 0$), then L/C and G/C (resp. L/C and R/C) can be determined from these data. We refer interested readers to [13], [14], [20].

The results of this paper extending previous works on lossless transmission lines to the case of general lossy lines constitute an important step towards practical applications of the IST to transmission line fault diagnosis.

Appendix

Proof of Proposition 2.

For arbitrary positive values a and b, the quantities $U(k,x), I(k,x)$, and $Z_0(x)$ of the extended circuit are well-defined for all $x \in (-a, l+b)$, where all the transformations and equations (7)-(9) remain valid. Thus the pair $\nu_1(k,x)$ and $\nu_2(k,x)$ is a solution to the Zakharov-Shabat equations (8) for $x \in (-a, l+b)$. Hence the solution is also valid for $x \in \mathbb{R}$ when a and b both tend to $+\infty$. Similarly to the proof of Proposition 2 in [12], we can show that (16a) holds by verifying that $\nu_1(k,x)$ and $\nu_2(k,x)$ as defined in (7) and extended to the whole real axis constitute a Jost solution of (8), up to a factor common to $\nu_1(k,x)$ and $\nu_2(k,x)$. The equality (16c) can be similarly proved.

Now let us prove (16b), which was not considered in [12]. When $b \to +\infty$, for all $x \in (l, +\infty)$, we have $R(x) = G(x) = 0$ and the characteristic impedance $Z_0(x) = Z_L$ is a constant. According to (9), the potential functions equal to zeros. Hence, the Zakharov-Shabat equations (8) become the following two decoupled first order differential equations

$$\frac{d\nu_1(k,x)}{dx} + ik\nu_1(k,x) = 0$$
$$\frac{d\nu_2(k,x)}{dx} - ik\nu_2(k,x) = 0$$

whose solutions are

$$\nu_1(k,x) = \nu_1(k,l)e^{-ik(x-l)} \tag{23a}$$
$$\nu_2(k,x) = \nu_2(k,l)e^{ik(x-l)} \tag{23b}$$

Similarly, for $x \in (-\infty, 0)$,

$$\nu_1(k,x) = \nu_1(k,0)e^{-ikx}$$
$$\nu_2(k,x) = \nu_2(k,0)e^{ikx}$$

From (13), combing with (7) and (3), we have

$$t(k) = \frac{\lim\limits_{x\to+\infty} \nu_2(k,x)e^{-ikx}}{\lim\limits_{x\to-\infty} \nu_2(k,x)e^{-ikx}}$$
$$= \frac{\nu_2(k,l)e^{-ikl}}{\nu_2(k,0)}$$
$$= \frac{[Z_L^{-\frac{1}{2}}U(k,l) + Z_L^{\frac{1}{2}}I(k,l)]e^{-ikl}}{[Z_S^{-\frac{1}{2}}U(k,0) + Z_S^{\frac{1}{2}}I(k,0)]}$$

$$= t_e(k)e^{-ikl}$$

Thus (16b) holds.

REFERENCES

[1] P. Smith, C. Furse, and J. Gunther, "Analysis of spread spectrum time domain reflectometry for wire fault location," *IEEE Sensors Journal*, vol. 5, pp. 1469–1478, December 2005.

[2] F. Auzanneau, M. Olivas, and N. Ravot, "A simple and accurate model for wire diagnosis using reflectometry," in *PIERS Proceedings*, August 2007.

[3] A. Lelong, L. Sommervogel, N. Ravot, and M. O. Carrion, "Distributed reflectometry method for wire fault location using selective average," *IEEE Sensors Journal*, vol. 10, pp. 300–310, 2010.

[4] L. A. Griffiths, R. Parakh, and C. F. B. Baker, "The invisible fray: A critical analysis of the use of reflectometry for fray location," *IEEE Sensors Journal*, vol. 6, pp. 697–706, June 2006.

[5] G. L. Lamb, *Elements of Soliton Theory*. New York: John Wiley & Sons, 1980.

[6] W. Eckhaus and A. Van Harten, *The inverse scattering transformation and the theory of solitons: an introduction*. Elsevier, 1981.

[7] H. E. Moses and C. M. de Ridder, "Properties of dielectrics from reflection coefficients in one dimension," Tech. Rep. 322, MIT Lincoln Laboratory, 1963.

[8] B. Gopinath and M. M. Sondhi, "Inversion of the telegraph equation and the synthesis of nonuniform lines," *Proceedings of the IEEE*, vol. 59, no. 3, pp. 383– 392, 1971.

[9] A. M. Bruckstein and T. Kailath, "Inverse scattering for discrete transmission-line models," *SIAM Review*, vol. 29, no. 3, pp. 359–389, 1987.

[10] M. Jaulent, "The inverse scattering problem for LCRG transmission lines," *Journal of Mathematical Physics*, vol. 23, pp. 2286–2290, December 1982.

[11] L. F. Knockaert, D. De Zutter, F. Olyslager, E. Laermans, and J. De Geest, "Recovering lossy multiconductor transmission line parameters from impedance or scattering representations," *IEEE transactions on Advanced Packaging*, vol. 25, no. 2, pp. 200–205, 2002.

[12] Q. Zhang, M. Sorine, and M. Admane, "Inverse scattering for soft fault diagnosis in electric transmission lines," *IEEE transactions on antennas and propagation*, accepted.

[13] M. Jaulent, "Inverse scattering problems in absorbing media," *Journal of Mathematical Physics*, vol. 17, pp. 1351–1360, 1976.

[14] P. V. Frangos and D. L. Jaggard, "Analytical and numerical solution to the two-potential Zakharov-Shabat inverse scattering problem," *IEEE transactions on antennas and propagation*, vol. 40, no. 4, pp. 399–404, 1992.

[15] S. J. Orfanidis, *Electromagnetic Waves and Antennas*. http: //www. ece. rutgers. edu/ orfanidi/ ewa/, 2008.

[16] P. V. Frangos and D. Jaggard, "A numerical solution to the Zakharov-Shabat inverse scattering problem," *IEEE transactions on antennas and propagation*, vol. 39, no. 1, pp. 74–79, 1991.

[17] P. V. Frangos and D. Jaggard, "Analytical and numerical solution to the two -potential Zakharov - Shabat inverse scattering problem," *IEEE transactions on antennas and propagation*, vol. 43, no. 6, pp. 547–552, 1995.

[18] G. Xiao and K. Yashiro, "An efficient algorithm for solving Zakharov-Shabat inverse scattering problem," *IEEE transactions on antennas and propagation*, vol. 50, no. 6, pp. 807 –811, 2002.

[19] H. Tang and Q. Zhang, "An efficient numerical inverse scateering algorithm for the Zakharav-Shabat equations with two potential functions." http://hal.inria.fr/inria-00447358/ or http://www.irisa.fr/sosso/zhang/TwoPotentialNumericalIST.pdf, 2009.

[20] P. V. Frangos, *One-dimensional inverse scattering: exact methods and applications*. PhD thesis, University of Pennsylvania, 1986.